Nat Hazards (2017) 87:1333–1359
DOI 10.1007/s11069-017-2820-8

ORIGINAL PAPER

Serviceability-related reliability for mainshock-damaged reinforced concrete piers considering the aftershock-induced seismic hazards

Chien-Kuo Chiu[1] · **Charles Poegoeh Arista**[1]

Received: 7 January 2016 / Accepted: 10 March 2017 / Published online: 1 April 2017

Abstract After the mainshock of an earthquake, the major concerns are their serviceability of damaged structures or safety when subjected aftershocks. How to choose the appropriate maintenance actions for damaged structures in their limited post-mainshock service periods is important. To consider the effect of aftershock events on the deterioration of structural performance, reduction factors of seismic capacity for specified damage states based on experimental data are used in the reliability analysis. Additionally, this work proposes an integral method that can analyze the time-dependent capacity of a mainshock-damaged RC pier and simulate aftershock events within a specified period after the mainshock of an earthquake, while at the same time considering cumulative damage induced by ground motions. To determine the post-mainshock service period for a mainshock-damaged RC pier located in a region with high seismic hazard induced by the aftershock, the proposed assessment method is applied to derive its reliability function of a specified damage state. Finally, the proposed procedure for the reliability function for a specified limit state is then applied to a case study of typical RC piers in Taiwan to demonstrate its applicability.

Keywords Reliability · Aftershock · Reduction factor · Reinforced concrete · Cumulative damage

1 Introduction

Losses from earthquakes can be disastrous. The scientific community has devoted a significant amount of effort to developing earthquake forecasting and warning systems, seismic design and retrofit technology, and disaster prevention and reduction systems.

✉ Chien-Kuo Chiu
ckchiu@mail.ntust.edu.tw

[1] Department of Civil and Construction Engineering, National Taiwan University of Science and Technology, Taipei, Taiwan

However, a well-constructed civil structure, which meets seismic design code, may still be damaged by an earthquake because design objectives allow for acceptable damage under large earthquakes. Furthermore, inspection and management of civil structures after the mainshock of an earthquake are challenging. The mainshock of an earthquake is typically followed by a number of aftershocks (usually smaller in magnitude) which occur in a limited area (i.e., the aftershock zone) around the epicenter of the mainshock. This sequence of aftershock events can last for months. Although these events are smaller in magnitude than the mainshock, they can be destructive.

When a large earthquake occurs, the residual seismic capacity of bridge or building will be determined based on the mainshock-induced damage levels. Additionally, post-mainshock deterioration of a structure due to a sequence of aftershocks may be an obstacle to re-occupancy. After the mainshock of an earthquake, the major concerns are their serviceability of damaged structures or safety when subjected aftershocks. How to choose and when to start the appropriate maintenance actions and for damaged structures in a post-earthquake period are important issues. Restated, decision variables (DVs) may be very dependent of post-mainshock performance of (possibly mainshock-damaged) structures in the aftershock environment when the rate of ground motion occurrence is high (Jalayer et al. 2011).

In general, to prevent damage and to repair a damaged community as rapidly as possible, engineers conduct post-earthquake/mainshock damage assessments immediately via site inspections of structural components. The main goal is to identify damaged structures and those in danger of collapse. For structures in Taiwan, damage is signified be a yellow or red tag, which warns people or prohibits access, respectively. Unless a building is totally damaged or collapsed, or the drift ratio exceeds the collapse criteria, engineers without a detailed financial loss estimation have difficulty deciding whether a building with badly damaged structural components is worth retrofitting or must be demolished. Based on some post-earthquake damage data for reinforced concrete (RC) residential buildings in Taiwan, Xue et al. (2009) linked inspection-determined component damage level, building damage state, and direct financial loss in terms of repair-to-replacement cost ratio. In the research conducted by Xue et al. (2009), damage to structural components are quantified by a set of damage factors, which are then integrated to create a building damage indicator. Additionally, the building repair-to-replacement cost ratio and story repair-to-replacement cost ratio for various damage levels of RC residential buildings have been estimated. With these statistical data, relationships between a building damage indicator and the repair-to-replacement cost ratio have been constructed from regression analysis by Xue et al. (2009). However, the damage factor (DF) of a structural component was not derived on the basis of the mechanical behavior of structural component. Obviously, DF is difficult to be applied to assess the residual seismic capacity of a structural component. However, reduction factors of seismic capacity for specified damage states are indispensable information to consider the effect of aftershock events on the deterioration of structural performance. Therefore, reduction factors of seismic capacity for RC members with specified damage states should be suggested on the basis of the experimental data. Additionally, for RC structures, how to simulate the cumulative damage induced by aftershock events for is still an inevitable problem in the post-earthquake maintenance. In brief, an assessment method that can be applied to derive the reliability function of a specified damage state for a mainshock-damaged RC structure located in a region with high seismic hazard induced by the aftershock is needed in the post-earthquake inspection and management of civil structures.

1.1 Literature review

Yeo and Cornell (2009) developed formal stochastic estimation models for expected financial loss over the lifetime of a building due to the mainshock and the subsequent aftershock sequence. In the reference (Yeo and Cornell 2009), mainshocks were typically modeled as a homogeneous Poisson process with a constant mean occurrence rate, while aftershocks were modeled as a non-homogeneous process with random magnitudes and parameters that were conditional on the random mainshock. However, almost every engineering system deteriorates over time due to exposure to extreme conditions and during routine use. Deterioration is a serious concern in engineering because it can considerably reduce the life and reliability of systems (Kumar and Gardoni 2014). Kumar and Gardoni (2014) proposed a novel probabilistic formulation for LCA of deteriorating systems named renewal theory-based life-cycle analysis (RTLCA). The RTLCA formulation was built based on renewal theory and proposes analytical solutions for the desired LCA variables using numerically solvable integral equations. Additionally, it can account for the accumulated seismic damage in the bridge columns caused by the earthquakes occurring during the bridge's life cycle. Taking a bridge for an example in Kumar and Gardoni (2014), the analysis results provided valuable insight into the importance of seismic damage in a bridge's life-cycle performance and the strategies to operate a system in an optimal manner.

Kumar et al. (2015) modeled the deterioration process as a combination of shock and gradual processes, which are independent of each other. The model proposed by Kumar et al. (2015) account for the effects of deterioration on both capacity of a system and the imposed demands on the system. The framework can account for two types of failure: demand exceeding capacity and accumulated damage exceeding allowable limit. Additionally, an accurate and computationally efficient semi-analytical solution and an approximate solution are proposed to estimate the time to failure. However, Kumar et al. (2015) excluded damage-dependent structural properties in the shock deterioration process.

For post-earthquake damage evaluation and retrofitting, the guidelines (JBDPA 2001) developed in 1991 were revised in 2001 based on lessons learned from disastrous earthquakes such as 1995 Hyogo-Ken-Nanbu (Kobe) earthquake (Maeda and Kang 2009; Chiu et al. 2014a). In the guidelines stated in JBDPA (2001), damage state categories for structural members are divided into five levels (Table 1). According to disastrous earthquakes in Japan, the damage states of vertical members in a building markedly influence a building's seismic capacity. Therefore, the guidelines identify and classify damage to columns and walls rather than to beams (Nakano et al. 2004). On the basis of the definition of each damage state (Table 1) stated in the research conducted by Maeda and Kang (2009) and Chiu et al. (2014a), Fig. 1 shows a ductile member deformed up to its maximum lateral strength after the yielding point of tensile rebars embedded in the member was reached. Obviously, after reaching maximum strength, the reduction in the strength of a ductile member is relatively small. Additionally, the damage state for a brittle member is similar to that of a ductile member up to maximum strength (Fig. 2). However, diagonal or X-shaped cracks may occur in damage levels I, II, and III. After maximum strength is reached, a significant reduction in both lateral and vertical strength may occur (damage level IV).

Table 1 Definition of damage levels for structural members (JBDPA 2001)

Damage level	Description of the corresponding damage state
I—Non-damage	Visible narrow cracks on concrete surface. Crack widths are less than 0.2 mm
II—Slight damage	Visible cracks on concrete surfaces. Cracks widths range from about 0.2 to 1 mm
III—Moderate damage	Noticeable wide cracks. Cracks widths range from about 1 to 2 mm. Localized crushing of concrete cover
IV—Severe damage	Crack widths are greater than 2 mm. Crushing of concrete with exposed reinforcing bars. Spalling of cover concrete
V—Total damage/collapse	Buckling of reinforcing bars. Crushing of core concrete. Visible vertical deformation in columns and/or shear walls. Side sway, subsidence of upper floors, and/or fracture of reinforcing bars are observes in some cases

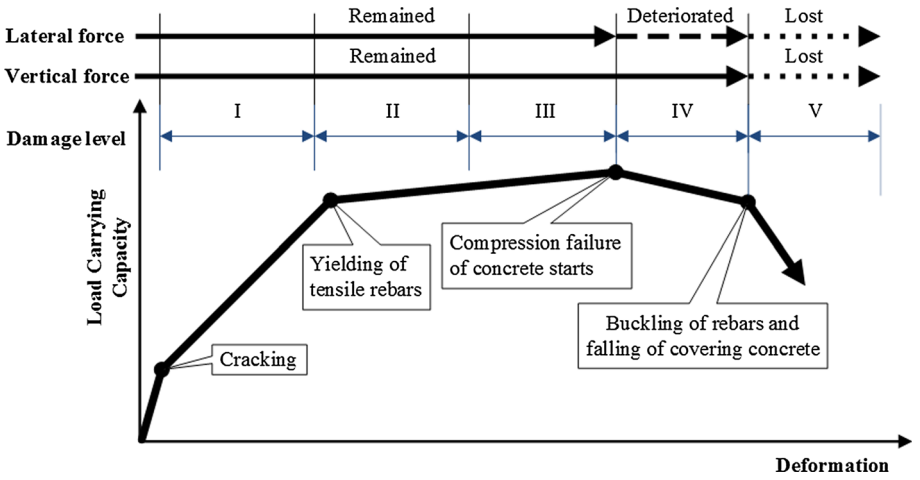

Fig. 1 Approximated lateral force–displacement relationships and damage levels for ductile members (JBDPA 2001)

1.2 Main purpose of this paper

The main purpose of this paper is to propose a seismic reliability assessment method for mainshock-damaged RC piers that can provide useful information to help engineers assess their safety or serviceability in a specified post-mainshock period. In the proposed method, reduction factors of seismic capacity for specified damage states are indispensable information for considering the effect of aftershock events on the deterioration of structural performance. However, according to the literature review, reduction factors of seismic capacity for RC bridge piers with specified damage states are still insufficient. In this work, experimental data for several full-size column specimens with various failure modes (flexural, flexural-shear, and shear failure) are used to suggest reduction factors of seismic capacity for specified damage states described in JBDPA (2001). While reduction factors of seismic capacity are defined based on the residual capacity of energy dissipation under

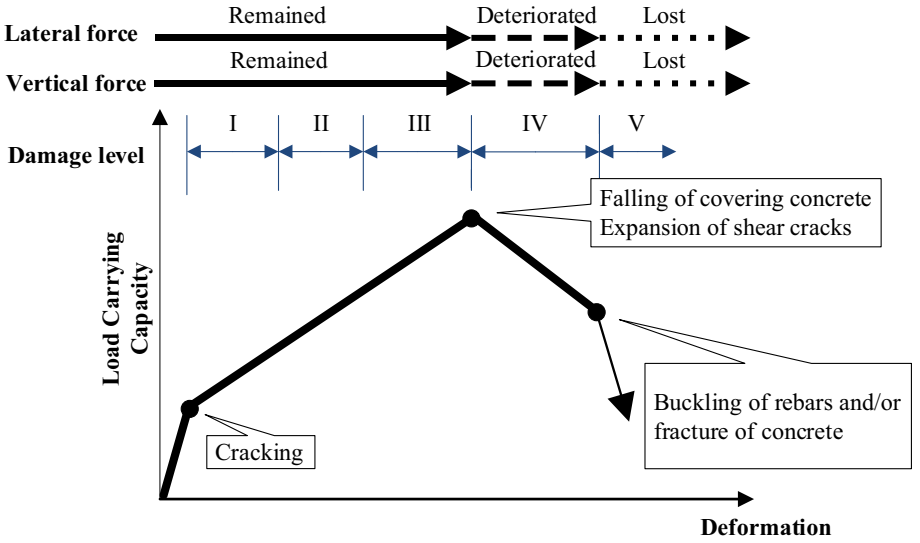

Fig. 2 Approximated lateral force–displacement relationships and damage levels for brittle members (JBDPA 2001)

cyclic loading, nonlinear dynamic analysis of a single-degree-of-freedom (SDOF) system for RC column specimens is conducted to discuss suggested reduction factors.

To identify the effect of aftershock events on the deterioration of structural performance, this work applies an integral simulation method. The proposed method can analyze the time-dependent structural capacity of a mainshock-damaged RC pier and simulate aftershock events within a specified period after the mainshock of an earthquake, while at the same time considering cumulative damage induced by ground motions. Compared with previous studies, this work considers the damage states induced by aftershock events in an earthquake are not independent. To consider the cumulative damage induced by aftershock events on the reliability function of a specified damage state, aftershock events are simulated and the Markov chain model is utilized to estimate the occurrence probability of a specified damage state. We assume the number of aftershocks follows Omori's law when analyzing the cumulative density function (CDF) of the magnitude of the aftershock within a specified post-mainshock period for an earthquake. Because a pier's structural capacity has several uncertainties, redactor factors of seismic capacity induced by the mainshock and aftershock, Monte Carlo simulation (MCS) is applied. Finally, the proposed procedure for the reliability function for a specified limit state is then applied to a case study of typical RC piers in Taiwan to demonstrate its applicability.

2 Seismic capacity reduction for damaged RC columns

Experimental data for RC column specimens are used to derive reduction factors of seismic capacity for damaged RC columns. Additionally, this work adopts nonlinear dynamic analysis for the SDOF system of each RC column specimen to verify the application of the suggested reduction factors of seismic capacity for damaged RC columns. For the

convenience of engineers, relationships between reduction factors, maximum residual cracking widths, and damage levels are also proposed.

2.1 Definition of reduction factors for damaged RC columns

According to Maeda et al. (2004), deterioration of seismic capacity for a damaged structural member can be estimated using energy dissipation capacity. Therefore, the reduction factor of seismic capacity for a damaged structural member can be defined as the ratio of residual capacity of energy dissipation to the initial capacity of dissipation energy (Fig. 3), and the reduction factor can be estimated using Eq. (1). For column specimens tested in a laboratory, the maximum response deformations under cyclic loading and the residual deformations during the unloading process can be observed to derive the dissipated energy. Then, a relationship between reduction factors of seismic capacity and residual deformations can be constructed using test results.

$$\eta = \frac{E_r}{E_d + E_r} = \frac{E_r}{E_t} \tag{1}$$

where η is the reduction factor of seismic capacity; E_d is dissipated energy; E_r is residual energy dissipation capacity; and E_t is original energy dissipation capacity ($E_d + E_r = E_t$).

For the convenience of engineers, reduction factors of seismic capacity should connect residual cracking widths with damage states of RC columns based on experimental data or analytical results. Maeda and Bunno (2001) suggested that a simplified geometric model can be used to simulate the relationship between maximum residual cracking widths and residual deformations for an RC column. Furthermore, they assumed the residual deformation of an RC column equals the sum of residual flexural deformation and residual shear deformation, which can be obtained from maximum residual shear and flexural crack widths, respectively, as in Eq. (2).

$$\delta = \delta_f + \delta_s = \frac{W_f^{max} n_f}{D - x} h + W_s^{max} n_s \cos\omega \tag{2}$$

where δ_f is the residual flexural deformation of a column; δ_s is the residual shear deformation of a column; W_s^{max} is the maximum residual shear crack width of a column

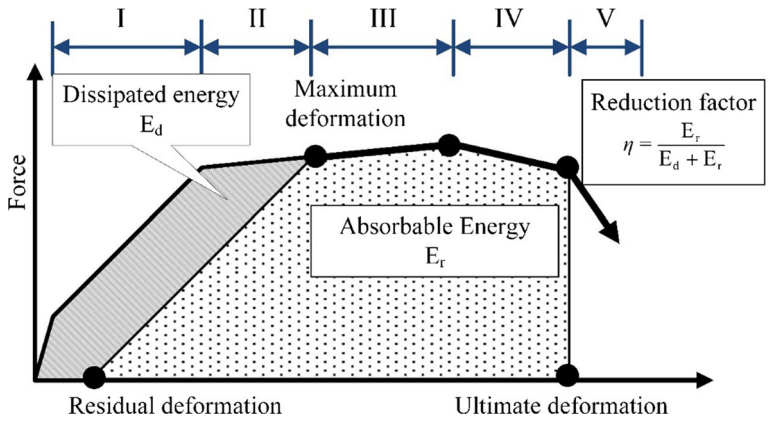

Fig. 3 Energy dissipation capacity of damaged structural members

(measured); W_f^{max} is the maximum residual flexural crack width of a column (measured); w is the angle between the shear crack and the vertical direction of column (45° is assumed herein); n_s is the ratio of total width of the residual shear crack to the maximum residual shear crack width ($\sum W_s/W_s^{max}$); n_f is the ratio of total width of the residual flexural crack to the maximum residual flexural crack width ($\sum W_f/W_f^{max}$); D is column depth; h is column clear height; and x is the distance from the most outside compression fiber to the neutral axis (0.2D is assumed herein).

Since the residual flexural deformation of an RC column can be approximately evaluated by the rigid body rotation (Maeda and Bunno 2001), the summation of residual flexural cracking widths measured in an RC column can be assumed equal to $R_f \times D$ (D is the depth of column; R_f is the residual flexural rotation angle and equal to $\frac{W_f^{max} n_f}{D-x}$) as shown in Fig. 4. Additionally, the summation of residual flexural cracking widths can also be estimated using the product of the maximum residual flexural cracking width and the parameter n_f, which means the ratio of the total width of residual flexural cracks to the maximum residual flexural cracking width, as shown in the first item of Eq. (2). For the residual shear deformation of an RC column, since the angle of shear crack is assumed to be 45°, it can be estimated using the product of the maximum residual shear cracking width and the parameter n_s, which means the ratio of the total width of residual shear cracks to the maximum residual shear cracking width, as shown in the second item of Eq. (2).

According to the research conducted by Choi et al. (2006), the total width of residual flexural/shear cracks and the maximum residual flexural/shear crack width tend to increase linearly with the peak drift ratio increasing after residual crack occurred, and the parameters n_f and n_s approximately are $D/2s$ (s is the spacing of transverse reinforcement).

2.2 Experimental data for RC column specimens

The work uses RC column specimens with various failure modes—flexural failure, flexural-shear failure, and shear failure—to identify reduction factors of seismic capacity. Experimental data are acquired from NCREE (National Center for Research on Earthquake Engineering, Taiwan) and JSCE (Japan Society of Civil Engineers, Japan), for 16 columns

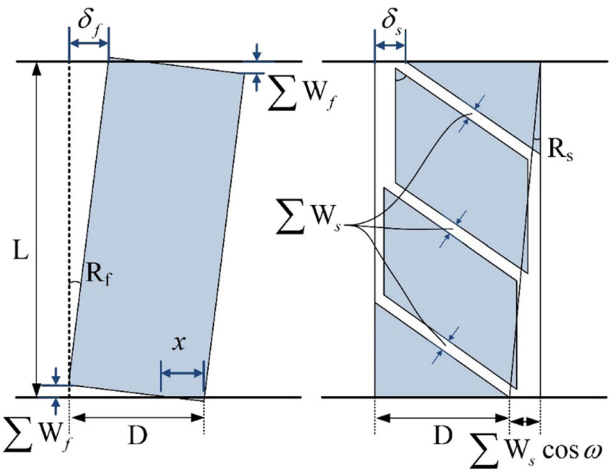

Fig. 4 Simplified crack-deformation model of column

(6 column specimens with flexural failure; 4 with shear failure; and 6 with flexural-shear failure). Table 2 lists the properties of all specimens. Table 3 shows yielding strength, yielding displacement, ultimate displacement, and ductility of each column specimen with flexural failure, i.e., BMRC1, NEWRC1, NEWRC2, NEWRC4, and NEWRC5.

2.3 Reduction factors of seismic capacity for damaged RC columns

For each specimen, residual and maximum drift ratios/deformations can be determined from its experimental lateral force–displacement curve, which are then used to define damage levels and their corresponding reduction factors of seismic capacity. Reduction factors decreased as residual drift ratios increased. Notably, seismic capacity of RC column specimens with shear failure declined significantly as residual drift ratios increased. Moreover, for any structure, columns with shear failure adversely affect its safety. Therefore, reduction factors of RC columns with shear failure should be determined conservatively. On the basis of the residual crack-deformation model in Sect. 2.1, residual deformations are utilized to calculate their corresponding maximum residual crack widths at various residual drift ratios.

According to the descriptions of damage states for RC columns (Table 1), maximum residual crack widths are used to classify damage levels on lateral force–displacement curves and estimate their corresponding seismic capacity reduction factors. Figure 5 shows the relationships between maximum residual crack widths and reduction factors for column specimens. These relationships can be important information for engineers when conducting post-mainshock inspections of damaged structures.

Compared to the reduction factors in Japan's guidelines (JBDPA 2001) for RC columns with flexural failure (Table 4a), the mean value of reduction factors in damage level I is smaller than the guideline's value, but the difference is insignificant. Additionally, the mean value of reduction factors corresponding to other damage levels is slightly higher than the guideline's values.

For RC columns with flexural-shear failure (Table 4b), the mean values of reduction factors obtained in this work are in the range of reduction factors for brittle and ductile members suggested in Japan's guideline, except for those in damage level I (JBPDA 2001). For RC columns with shear failure (Table 4c), the mean values of reduction factors obtained in this work exceed the guideline's values, except for those in damage level I. Because shear failure of a column may adversely affect the safety of the entire structure, we suggest using a reduction factor for damage level IV of zero, which is the same as in Japan's guideline. Therefore, on the basis of the experimental data, we suggest modified reduction factors for the seismic capacity for damaged RC columns with various failure modes (Table 5). The following section uses nonlinear dynamic analyses of an SDOF system for specimens to investigate the application of the suggested reduction factors.

2.4 Reduction factor of seismic capacity defined by nonlinear dynamic analysis

To investigate reduction factors of seismic capacity for RC column specimens, nonlinear dynamic analysis was applied. In this analysis, we assume when a specified ground motion causes an RC column without any damage to have damage level V (total damage or collapse), the intensity of ground motion can be regarded as the original seismic capacity of the column, A_{do}. Furthermore, two sequential ground motions are applied to an RC column specimen to investigate its residual seismic capacity: The first ground motion

Table 2 Properties of all selected specimens

Parameters of specimen	Name of specimen					
	BMRC1	NEWRC1	NEWRC2	NEWRC4	NEWRC5	JSCE24
(*a*) *Column specimens with flexural failure*						
Width (cm)	60	50	50	50	50	50
Depth (cm)	60	50	50	50	50	50
Clear height (cm)	360	360	360	360	360	215
Thickness of concrete cover (cm)	4	4	4	4	4	4
Compressive strength of concrete (MPa)	37.4	82.5	82.5	82.5	82.5	–
Yielding stress of longitudinal reinforcement (MPa)	544.3	750.5	750.5	750.5	750.5	–
Yielding stress of transverse reinforcement (MPa)	347.6	828.5	828.5	828.5	347.6	–
Diameter of longitudinal reinforcement (cm)	2.54	2.54	2.54	2.54	2.54	2.2 and 1.3
Diameter of transverse reinforcement (cm)	1.27	1.27	1.27	1.27	1.27	0.6
Spacing of transverse reinforcement (cm)	10	10	20	10	10	13
Number of longitudinal reinforcement	16	12	12	12	12	12–2.2 and 16–1.3
Number of transverse reinforcement (*X* direction)	5	4	4	4	4	2
Number of transverse reinforcement (*Y* direction)	5	4	4	4	4	2
Axial load (kg)	136,000	136,000	136,000	272,000	136,000	–

Parameters of specimen	Name of specimen					
	JSCE02	JSCE03	JSCE04	JSCE05	JSCE14	JSCE20
(*b*) *Specimen columns with flexural-shear failure*						
Width (cm)	90	90	40	40	50	125
Depth (cm)	40	40	40	40	50	40
Clear height (cm)	100	100	124.5	124.5	235	190
Thickness of concrete cover (cm)	4	4	4	4	2	2
Diameter of longitudinal reinforcement (cm)	1	1	1.3	1.3	1	1
Diameter of transverse reinforcement (cm)	0.6	0.6	0.6	0.6	0.6	0.6
Spacing of transverse reinforcement (cm)	15	15	7	7	25	12
Number of longitudinal reinforcement	34	38	20	20	56	66
Number of transverse reinforcement (*X* direction)	6	6	2	2	4	2
Number of transverse reinforcement (*Y* direction)	2	2	2	2	4	2

Table 2 continued

Parameters of specimen	Name of specimen			
	A1	A2	A3	A4
(*c*) *Column specimens with shear failure*				
Width (cm)	60	60	60	60
Depth (cm)	60	60	60	60
Clear height (cm)	180	180	180	180
Thickness of concrete cover (cm)	4	4	4	4
Compressive strength of concrete (MPa)	94.3	101.8	98.7	109.2
Yielding stress of longitudinal reinforcement (MPa)	749.3	749.3	749.3	749.3
Yielding stress of transverse reinforcement (MPa)	878.7	878.7	878.7	878.7
Diameter of longitudinal reinforcement (cm)	3.22	3.22	3.22	3.22
Diameter of transverse reinforcement (cm)	1.27	1.27	1.27	1.27
Spacing of transverse reinforcement (cm)	45	45	26	26
Number of longitudinal reinforcement	16	16	16	16
Number of transverse reinforcement (*X* direction)	3	3	3	3
Number of transverse reinforcement (*Y* direction)	3	3	3	3
Axial load (kg)	339,000	367,000	355,000	393,000

Table 3 Experimental results for BMRC1, NEWRC1, NEWRC2, NEWRC4, and NEWRC5

Name of specimen	F_y (kN)	δ_y (cm)	δ_u (cm)	Ductility (μ)
BMRC1	351.76	4.98	28.8	5.8
NEWRC1	286.57	5.89	32.4	5.5
NEWRC2	267.18	5.88	21.6	3.7
NEWRC4	314.01	4.94	28.8	5.8
NEWRC5	279.87	6.21	36.0	5.8

causes the specified damage state, and the second ground motion is used to cause the column to collapse or be totally damaged. Then, the intensity of the second ground motion can be regarded as the residual seismic capacity of the column with a specified damage state, A_{di}. Compared to its original seismic capacity, the reduction factor of seismic capacity can be derived as

$$\eta_{dyn} = \frac{A_{di}}{A_{do}} \tag{3}$$

In nonlinear dynamic analysis of an RC column, a hysteretic law is needed to describe its hysteretic behavior. The first such law was proposed by Clough et al. (1965). A refined hysteresis model was proposed by Takeda (Takeda et al. 1972). In the Takeda model, monotonic behavior is described by a trilinear skeleton curve which accounts for concrete cracking and reinforcing steel yielding. Moreover, hysteretic behavior is described by a number of rules for unloading and reloading, and it is based on data obtained from specimens tested in an earthquake simulator. However, failure or extensive damage caused by shear or bond deterioration was not considered in the model; that is, the Takeda model, similar to the Clough model, simulates only flexural behavior.

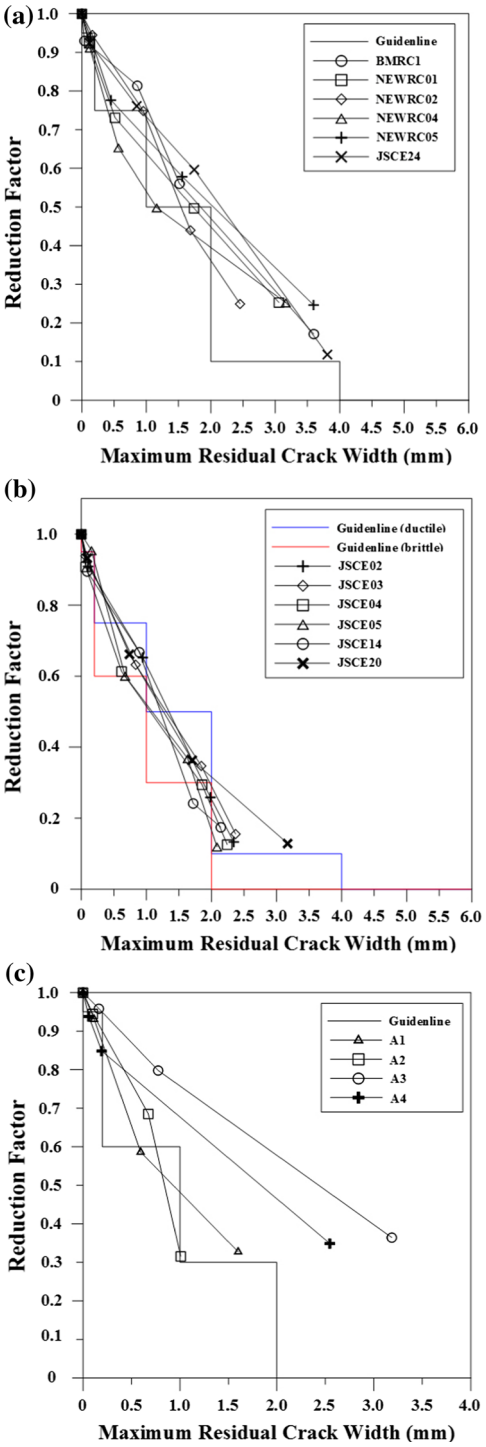

Fig. 5 Relationship between maximum residual crack widths and reduction factors for column specimens with various failure modes. **a** Flexural failure, **b** flexural-shear failure, and **c** shear failure

Table 4 Reduction factors for seismic capacity of column specimens with various failure modes

Damage level	Mean	Mean + 1σ	Mean − 1σ	Guideline (ductile)
(*a*) *Flexural failure*				
Initial	1.00	1.00	1.00	*1.00*
I	0.93	0.94	0.92	*0.95*
II	0.75	0.80	0.70	*0.75*
III	0.53	0.59	0.47	*0.50*
IV	0.22	0.27	0.16	*0.10*
V	0.00	0.00	0.00	*0.00*

Damage level	Mean	Mean + 1σ	Mean − 1σ	Guideline (ductile)	Guideline (brittle)
(*b*) *Flexural-shear failure*					
Initial	1.00	1.00	1.00	*1.00*	*1.00*
I	0.92	0.95	0.90	*0.95*	*0.95*
II	0.64	0.67	0.61	*0.75*	*0.60*
III	0.31	0.37	0.26	*0.50*	*0.30*
IV	0.14	0.16	0.12	*0.10*	*0.00*
V	0.00	0.00	0.00	*0.00*	*0.00*

Damage level	Mean	Mean + 1σ	Mean − 1σ	Guideline (brittle)
(*c*) *Shear failure*				
Initial	1.00	1.00	1.00	*1.00*
I	0.94	0.96	0.93	*0.95*
II	0.73	0.85	0.61	*0.60*
III	0.34	0.36	0.32	*0.30*
IV	0.00	0.00	0.00	*0.00*
V	0.00	0.00	0.00	*0.00*

Flexural failure The flexural failure mode of a column occurs when the flexural capacity is less than 60 % of shear capacity

Flexural-shear failure The flexure-shear failure mode of a column occurs when shear force related to flexural capacity exceeds 60 % of shear capacity and is less than the shear capacity

Shear failure The shear failure mode of a column occurs when flexural capacity exceeds shear capacity

Table 5 Suggested reduction factors for seismic capacity of damaged RC columns

Damage level	Flexural failure	Flexural-shear failure	Shear failure
Initial	1	1	1
I	0.9	0.9	0.9
II	0.7	0.6	0.6
III	0.5	0.3	0.3
IV	0.1	0.1	0
V	0	0	0

The Takeda model is adopted for nonlinear dynamic analysis of the residual deformation response corresponding to a ground motion for the SDOF system of an RC column member. Several parameters are needed to define the Takeda model (Fig. 6): initial elastic stiffness, k_y;

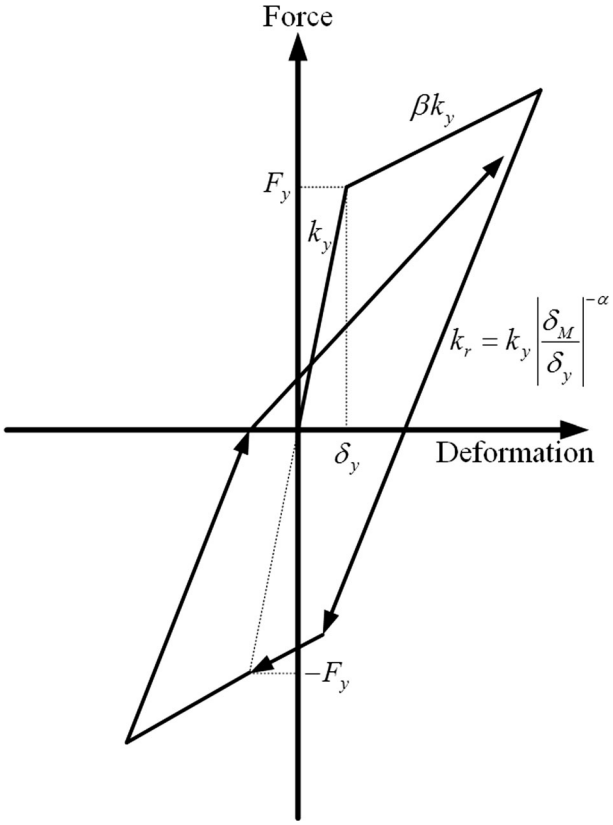

Fig. 6 Hysteretic behavior in the Takada model

ratio of post-yielding stiffness to initial elastic stiffness, β; yielding strength, F_y; and the unloading stiffness degradation parameter, α. For each column specimen, these parameters are identified using experimental results. Notably, the unloading stiffness of the adopted model is reduced by an exponential function of the previous maximum deformation response.

In this work, acceleration time histories recorded in the Chi–Chi earthquake are used as ground motions in nonlinear dynamic analysis. To investigate the ground motion effect on reduction factors of seismic capacity, nine of the acceleration time histories are chosen from measurement stations TAP003, TAP005, TAP008, KAU062, TCU052, TTN046, CHY050, ILA050, and HWA051. Additionally, all acceleration time histories are modified, such that they are compatible with the elastic design response spectrum suggested in Taiwan's seismic design code (MOI 2005) (Fig. 7). This work performs only nonlinear dynamic analysis for RC column specimens with flexural failure, which is most common failure mode in RC bridge piers. Taking the measurement stations TAP003, TAP005, TAP008, KAU062, HWA051, and TCU052 for example, Fig. 8 shows the reduction factors of seismic capacity obtained from nonlinear dynamic analysis. According to the simulation results, the reduction factors are slightly higher than suggested factors (Table 5), regardless of ground type. That is, engineers can use the reduction factors of seismic capacity in Table 5 to obtain a conservative residual seismic capacity for damaged RC columns for post-mainshock inspection.

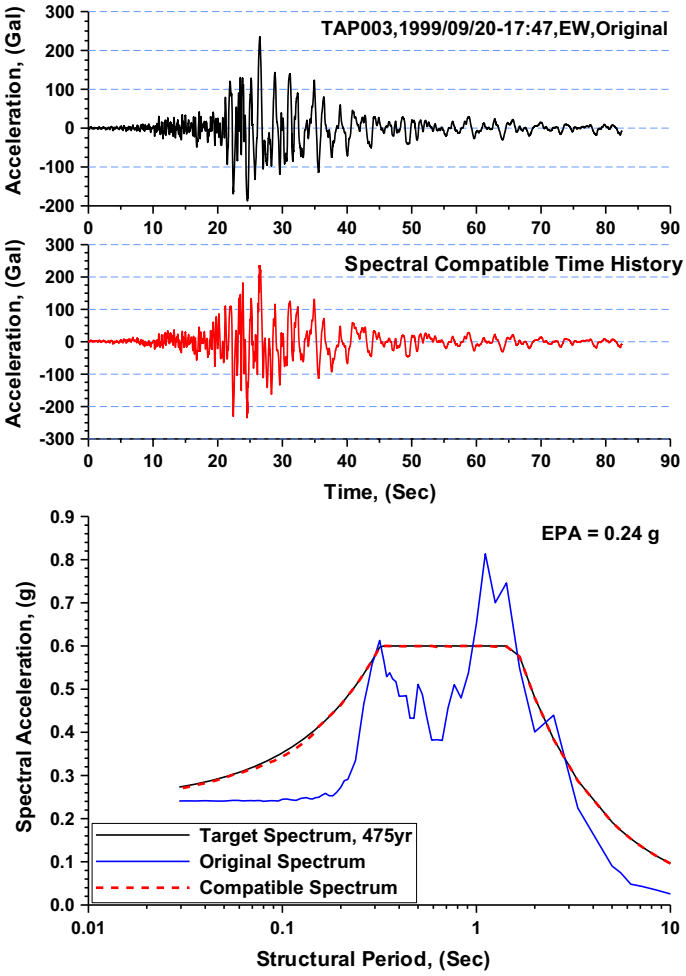

Fig. 7 Acceleration time history of ground motion from TAP003 (19990921, $M_L = 7.3$)

3 Seismic reliability of main-shocked RC piers subjected to aftershocks

An integral simulation procedure, which is based on the Markov chain model, is applied to acquire the post-mainshock reliability function of safety or serviceability, which is related to an acceptable limit state for an RC pier in seismically active zones. Based on the post-mainshock reliability function of safety or serviceability, engineers can understand the effect of cumulative damage associated with aftershocks. Restated, the simulated reliability function data can improve resource allocation and asset management.

3.1 Method for simulating the aftershock

Generally, calculating cumulative damage due to aftershocks requires knowledge of the number of events and their magnitudes that will likely occur with each earthquake within a given time window. The number of aftershocks in a given period depends on knowledge of

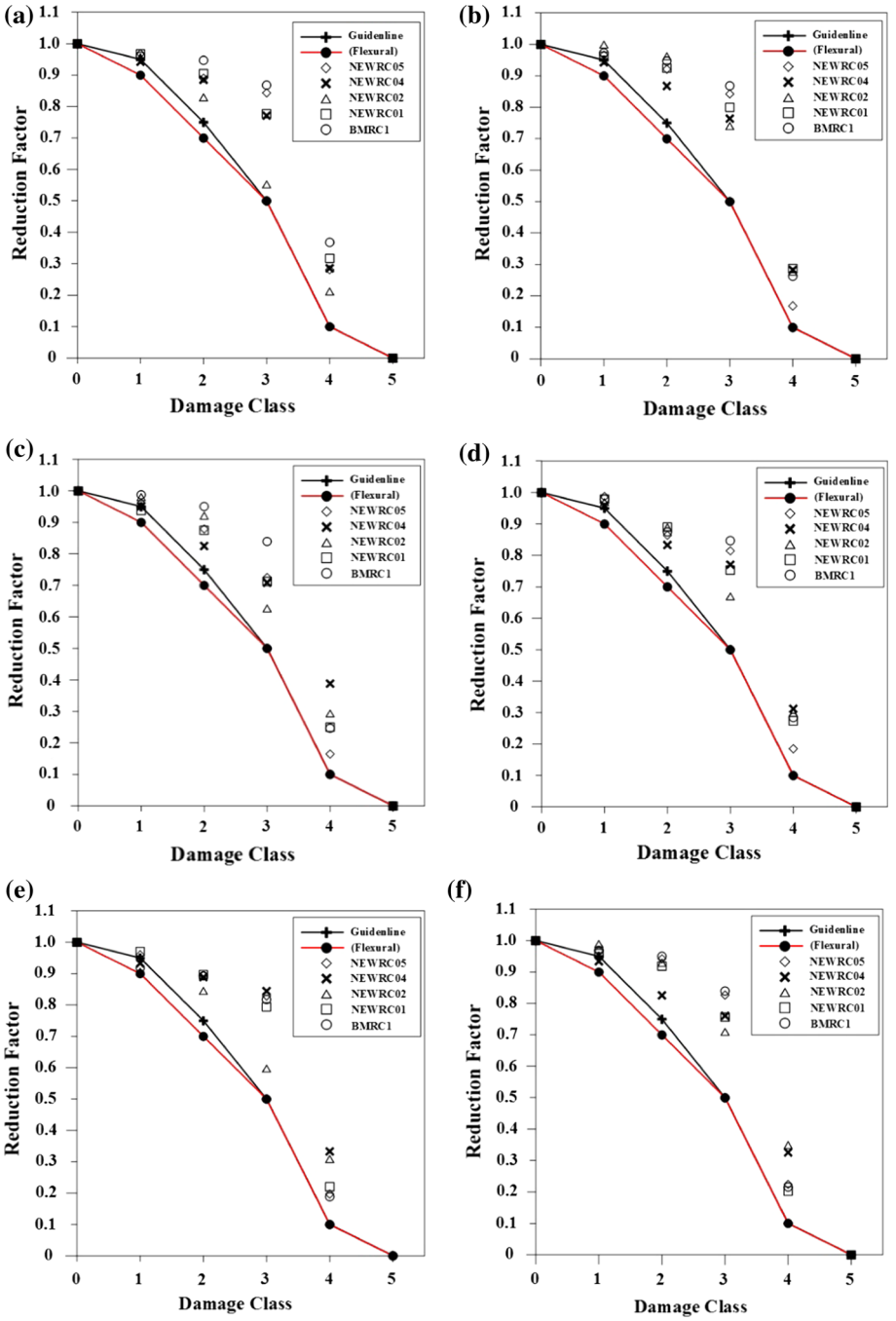

Fig. 8 Residual factors of seismic capacity from nonlinear dynamic analysis

the time rate of aftershocks. For convenience, the aftershock sequence can be modeled using a non-homogeneous Poisson process, and the time-decaying rate of aftershocks is modeled by modified Omori's law (Utsu 1961):

$$n(t) = \frac{K}{(t+c)^p} \tag{4}$$

$$N_o(t) = \int_t^{t+7\text{days}} n(t)\mathrm{d}t \tag{5}$$

where $n(t)$ is total (daily) number of aftershocks at time t after the mainshock and K, p, and c are constants. Additionally, the magnitude distribution for aftershocks is modeled using the Gutenberg–Richter law (G–R law; Eq. 6):

$$\log N = a - b \times m \tag{6}$$

$$F(m) = \frac{N_o(t) - N(m)}{N_o(t)} \tag{7}$$

where N is the number of events with a magnitude $\geq m$ and a and b are constants.

According to the research (MOTC 2011), Eq. (5) can be used to estimate the number of aftershocks within a specified period after the mainshock, N_o. Then, using the same slope value of the G–R law, b, parameter a can be defined as $\log N_o$. Restated, the G–R law for aftershocks within a specified period can be generated. Furthermore, the number of aftershocks, N_o, can be set at 1.0 to obtain the maximum magnitude of aftershocks within a specified period. For a specified period after the mainshock, the CDF of aftershock magnitude can be generated based on maximum magnitude and number of aftershocks, as in Eq. (7).

Based on Eq. (7) and the attenuation law of ground acceleration, Y_r, suggested in the research [Campbell 1981; (Eq. 8)], this work simulates using MCS the magnitude of aftershocks and their corresponding spectral accelerations within a specific period after the mainshock for a structure.

$$Y_r = f(m,R) = C_1 e^{C_2 m}\left[R + C_4 e^{C_5 m}\right]^{-C_3} \tag{8}$$

where C_1, C_2, C_3, C_4, and C_5 are constants, which can be obtained using the regression analysis; R is the distance between the epicenter and structure's site (km).

3.2 Cumulative damage evaluation using the Markov chain model

After the mainshock of an earthquake, a structure may be damaged to varying states. If this damage is not repaired, the likelihood of the structure being further damaged by subsequent ground motion increases. Damage can be classified into several damage states, such as no damage, light damage, moderate damage, severe damage, and total collapse (Table 1). A structure either remains in the same state or moves to another state after each ground motion. Therefore, according to the Markov chain model suggested by Chiu (2014a, b), simulated probabilities determine the likelihood of a structure being in a particular damage state after a number of ground motions or at a future time.

3.2.1 The Markov chain model

The Markov chain model (Ang and Tang 1984) is a stochastic process, a mathematical model for a system or an element that has random outcomes. These outcomes are considered a function of an independent variable such as a temporal or spatial factor. For a discrete parameter Markov chain model, transitional probability from state i at time t_m to state j at time t_n is derived by Eq. (9). The Markov chain model is homogeneous when $p_{i,j}(m,n)$ depends only on the difference between t_n and t_m; in this work, Eq. (10), which is the k-step transition probability function, can be defined. Additionally, a transition probability matrix can be generated by summing the transition probabilities for a system with m states, as in Eq. (11).

$$p_{i,j}(m,n) = P(X_n = j | X_m = i); n > m \tag{9}$$

$$p_{i,j}(k) = P(X_k = j | X_0 = i) = P(X_{k+s} = j | X_s = j); s \geq 0 \tag{10}$$

$$P_T = \begin{pmatrix} p_{1,1} & \cdots & p_{1,m} \\ \vdots & \ddots & \vdots \\ p_{m,1} & \cdots & p_{m,n} \end{pmatrix} \tag{11}$$

The probabilities of the initial states of a system can be listed in a row matrix, as in Eq. (12). In matrix notation, the n-stages state probabilities can be expressed by Eq. (13).

$$P(0) = [p_1(0), p_2(0), \ldots, p_m(0)] \tag{12}$$

$$P(n) = p(0)p_{\mathrm{T}}^n \tag{13}$$

where $p_i(0)$ is the probability that a system is initially in state i. In the special case for which the initial state of a system is known, such as at state i, then $p_i(0) = 1.0$ and all other elements in the row matrix, $P(0)$, are zero.

In the homogeneous Markov chain model, transition probabilities depend only on current states, not on time. However, this is an assumption and it is questionable for a structure because seismic hazard of aftershocks varies over time. Therefore, to predict post-earthquake seismic reliability for a structure while considering the seismic hazard of aftershocks, this work adopts the non-homogeneous Markov chain model. Restated, the transition probability matrix, P_{T}, varies over time and can be a specific period after the mainshock of an earthquake.

3.2.2 Transition probability matrix of seismic structural damage

When the estimated damage state of a structure after a ground motion event exceeds the limiting value of a specified damage state, one can assume the estimated damage state of the structure exceeds it specified damage state. According to the suggestion stated in Chiu (2014a, b), by incorporating uncertainty into aftershock events, as well as into structural capacity, the exceedance probabilities for different damage states, P_{SE}, can be estimated using MCS (Eq. 14) in this work. Each uncertainty considered in this work is characterized in Sect. 3.2.3.

$$p_{\mathrm{SE}}\left(\delta_{\mathrm{r}}^{\mathrm{lim}}\right) = P\left[\left(\delta_{\mathrm{r}} - \delta_{\mathrm{r}}^{\mathrm{lim}}\right) > 0\right] \tag{14}$$

where $\delta_{\mathrm{r}}^{\mathrm{lim}}$ is the limiting width of residual cracks for a specified damage state (cm).

We assume an RC pier damaged by a previous ground motion event experiences additional ground motion events. Because seismic structural damage is not repaired, the structural properties (i.e., stiffness and yielding deformation) of a pier must be modified based on maximum deformation response on the basis of the research conducted by Chiu et al. (2014b). For example, when an RC pier with a specified damage state is not repaired before the next ground motion event, residual deformation corresponding to the damage state and modification to its structural properties are considered when estimating the damage state for the next ground motion.

After modifying the structural properties, except for yielding base shear force, which we assume remains constant, elastic stiffness and yielding deformation must be recalculated based on maximum deformation response corresponding to the previous ground motion event, $\delta_{\mathrm{M}}^{1\mathrm{st}}$. Additionally, maximum deformation response, $\delta_{\mathrm{M}}^{1\mathrm{st}}$, can be estimated using residual seismic capacity, $\eta \times E_{\mathrm{T}}$ (Fig. 9) as in Eq. (15), which is derived assuming the post-mainshock/aftershock dissipation energy capacity equals $\eta \times E_{\mathrm{T}}$, where η is the reduction factor of seismic capacity corresponding to a specified damage state, and E_{T} is the original dissipation energy capacity. Additionally, we assume elastic stiffness after a ground motion event, $k_{\mathrm{y}}^{1\mathrm{st}}$, becomes less than the original elastic stiffness and can be modified using Eq. (16). The yielding deformation, $\delta_{\mathrm{y}}^{1\mathrm{st}}$, can be represented by $\delta_{\mathrm{r}}^{1\mathrm{st}} + \frac{F_{\mathrm{y}}}{k_{\mathrm{r}}^{1\mathrm{st}}}$. If maximum response deformation does not exceed yielding deformation, structural properties can be assumed the same as the original properties.

$$\delta_{\mathrm{M}}^{1\mathrm{st}} = 2\delta_{\mathrm{u}} - \delta_{\mathrm{r}}^{1\mathrm{st}} - \left(\frac{2\eta E_{\mathrm{T}}}{F_{\mathrm{y}}}\right) \tag{15}$$

$$k_{\mathrm{r}}^{1\mathrm{st}} = \frac{F_{\mathrm{y}}}{\delta_{\mathrm{M}}^{1\mathrm{st}} - \delta_{\mathrm{r}}^{1\mathrm{st}}} \tag{16}$$

where F_{y} is the original yielding base shear force (kN); k_{y} is the original elastic stiffness; and δ_{u} is the original ultimate deformation capacity (cm).

To estimate the maximum deformation response and residual deformation associated with the next ground motion event, $\delta_{\mathrm{M}}^{2\mathrm{nd}}$ and $\delta_{\mathrm{r}}^{2\mathrm{nd}}$, while considering the modified structural

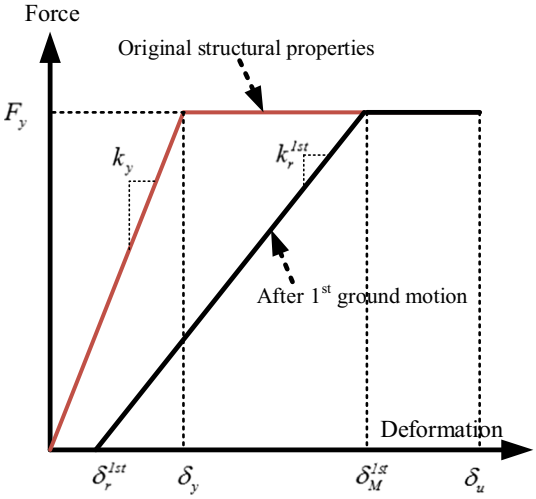

Fig. 9 Concept of modification of structural properties

properties for an RC pier with seismic structural damage, as in Eqs. (17) and (18), this work applies the equivalent energy method.

$$\delta_{\mathrm{M}}^{2\mathrm{nd}} = \frac{1}{2}\left(\delta_{\mathrm{M}}^{1\mathrm{st}} + \delta_{\mathrm{r}}^{1\mathrm{st}} + \left(\frac{2MS_{\mathrm{a}}}{F_{\mathrm{y}}}\right)\right) \tag{17}$$

$$\delta_{\mathrm{r}}^{2\mathrm{nd}} = \delta_{\mathrm{r}}^{1\mathrm{st}} + \left(\delta_{\mathrm{M}}^{2\mathrm{nd}} - \delta_{\mathrm{M}}^{1\mathrm{st}}\right) \tag{18}$$

where S_{a} is the response spectral acceleration of an aftershock (g) and M is the equivalent mass of the SDOF system for an RC pier (kg).

To build a transition probability matrix for an RC pier, we assume an RC pier has already been damaged by a ground motion of an earthquake to a specific damage state. Its maximum residual crack width is assumed to be a uniform distribution in the range of limiting values for the specific damage state. Based on Eqs. (15)–(18) and their corresponding uncertainties, transition probabilities from the specific damage state to other damage states, which are equal to or more severe than the initial damage state, can be derived via MCS. Following the same simulation procedure (Fig. 10), the transition probability matrix, P_{T}, can be constructed. Additionally, when repair work is not performed after the mainshock and aftershocks, the occurrence probability of each damage state can be estimated using the Markov chain model, which sets occurrence times of aftershocks within a specified period.

3.2.3 *Uncertainties considered in the assessment procedure for the post-mainshock reliability function of safety or serviceability*

Uncertainties associated with aftershocks, structural capacity, and seismic structural damage induced by a ground motion must be considered when estimating a structure's post-mainshock seismic reliability in this work. Uncertainty related to aftershocks is

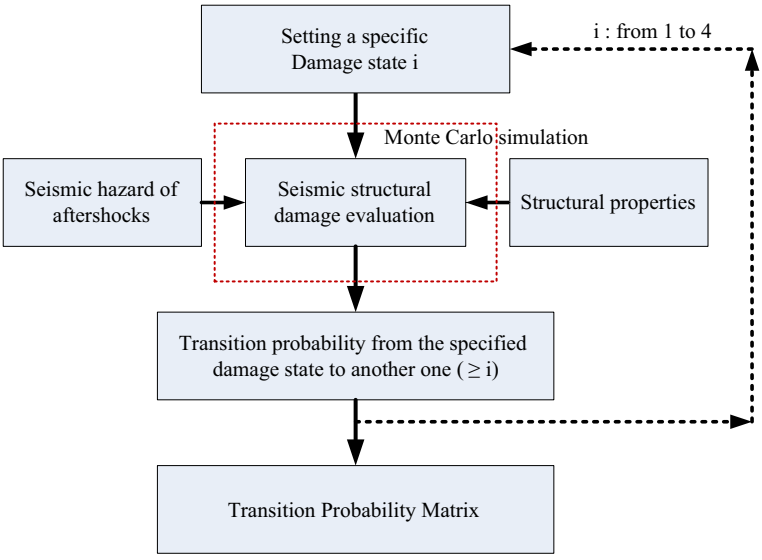

Fig. 10 Simulation procedure for the transition probability matrix

included in the location and magnitude, m. In this work, aftershocks recorded in the Chi–Chi earthquake are used to generate a hazard curve of magnitude of aftershocks, as in Sect. 3.1. In addition to the hazard curve of the magnitude of aftershocks, the distance between an aftershock's location and the structure's site is assumed to have a uniform distribution, reflecting the uncertainty of ground motion of an aftershock when estimating the transition probability matrix for an RC pier, which is needed by the Markov chain model.

Uncertainty related to structural properties is included in ultimate deformation capacity, δ_u, yielding strength, F_y, and elastic stiffness, k_y, of the SDOF system for an RC pier. Because this uncertainty is altered by material properties, the structural system, and construction process, estimating this uncertainty is difficult. In the case study, Table 6 lists the assumed uncertainty related to structural properties. However, for various types of bridge, this uncertainty can be defined accurately based on engineers' experience.

This work accounts for uncertainty in seismic structural damage induced by a ground motion that is related to maximum residual crack width and a reduction factor corresponding to a specified damage state. For a specific damage state, we assume maximum residual crack width has a uniform distribution. Additionally, based on experimental data (Sect. 2.4), we assume the redactor factor corresponding to the specific damage level has a normal distribution with 0.1 as the coefficient of variation (Table 4).

4 Case study

Three typical simply supported bridges supported by circular piers, selected from standard design drawings by Taiwan Highway Burea, were utilized to demonstrate the applicability of the proposed assessment method. The bridge design adopted from AASHTO Standard Specifications for Highway Bridges (American Association of State Highway and Transportation Officials, AASHTO), 1977, with horizontal seismic coefficient of 0.15 for calculating the longitudinal and lateral reinforcements. Table 7 demonstrates the design parameters for the case-study bridges. The summation of all self-weight of all components on the superstructure has been reported on the stand design drawing, as the vertical load transferring to the top of pier, so that to obtain the axial force at the bottom of pier by including self-weight of cap-beam and pier stem. The axial load coefficient is 0.06, 0.08, and 0.11, respectively, corresponding to the product of specified concrete strength and gross area.

The seismic performance of the bridges was simulated by a theoretical approach, resulting in a relationship of lateral force and top displacement of the pier. The analytical results of effective yielding moment, yielding curvature, as well as ultimate moment and ultimate curvature were extracted from the section analysis and provided as the basis to

Table 6 Uncertainties of structural properties considered in the proposed assessment procedure

Uncertainty	Statistical properties
Yielding deformation (δ_y)	Lognormal distribution with 0.1 as the coefficient of variation
Yielding strength (F_y)	Lognormal distribution with 0.1 as the coefficient of variation
Ultimate deformation capacity (δ_u)	Lognormal distribution with 0.15 as the coefficient of variation

Table 7 Design parameters for the case-study bridges

Design parameters	Bridge1 (RCP-4510)	Bridge2 (RCP-4523)	Bridge3 (RCP-4525)
Span (m)	20	30	40
Width (m)	9	9	9
Height (m)	14	11	10
Diameter (cm)	250	240	250
Cover (cm)	7	7	7
Specified compressive strength of concrete (MPa)	21	21	21
Yielding strength of longitudinal reinforcement (MPa)	409	409	409
Yielding strength of transverse reinforcement (MPa)	384	384	384
Diameter of longitudinal reinforcement (cm)	3.2	3.2	3.2
Diameter of transverse reinforcement (cm)	1.6	1.6	1.6
Number of longitudinal reinforcement	54	54	74
Spacing of transverse reinforcement (cm)	10	10	10
Self-weight of superstructure (kg)	260,000	426,000	660,000
Self-weight of substructure (kg)	383,310	343,570	431,930
Total weight of the structure (kg)	643,310	769,570	1091,930
Plastic hinge length (cm)	140.79	116.79	108.79
Yielding displacement (cm)	10.91	7.18	5.92
Ultimate displacement (cm)	84.65	55.03	39.52

calculate the yielding displacement and ultimate displacement, based on the first moment-area theorem and plastic hinge length. It is assumed no buckling failure and no shear failure participated in the member; that is, only flexural behavior is the major contribution to the displacement calculation of a single pier. In addition, the moment capacity divided by the height of pier is recognized as the lateral strength corresponding to yielding and ultimate stage. Figure 11 presents the pushover curves of three case-study bridges mentioned above (named as RCP-4510, RCP-4523, and RCP-4525, respectively). The shortest span of the bridge provides the smallest strength but largest displacement. The displacement ductility, defined as ultimate displacement divided by yielding displacement, for selected piers is 7.8 (RCP-4510), 7.7 (RCP-4523), and 6.8 (RCP-4525), respectively. The pushover curves of each SDOF system are further transforming into Acceleration–Displacement Response Spectrum (ADRS) by ATC-40 procedure (ATC 1996), as shown in Fig. 12.

According to the investigation conducted by MOTC (2011), aftershocks recorded in Chi–Chi earthquake mostly occurred in the five regions (A, B, C, D, and E). In the region A near Puli of Nantou in Taiwan, which is about 10 km far from the epicenter of Chi–Chi earthquake, the occurrence times and magnitude of aftershocks are larger than other regions. Therefore, we assume the selected RC piers are located in Puli of Nantou. Additionally, because the location of aftershocks is not easy to be specified, we assume aftershock events are uniformly located in the range of 0.5, 1.0, 3.0, and 5.0 km from the structure's site, respectively. The damage state induced by mainshocks for the selected RC piers is set at damage levels I, II and III to discuss their corresponding reliability functions for a specified damage state. Generally, for a damaged RC pier, when its damage state

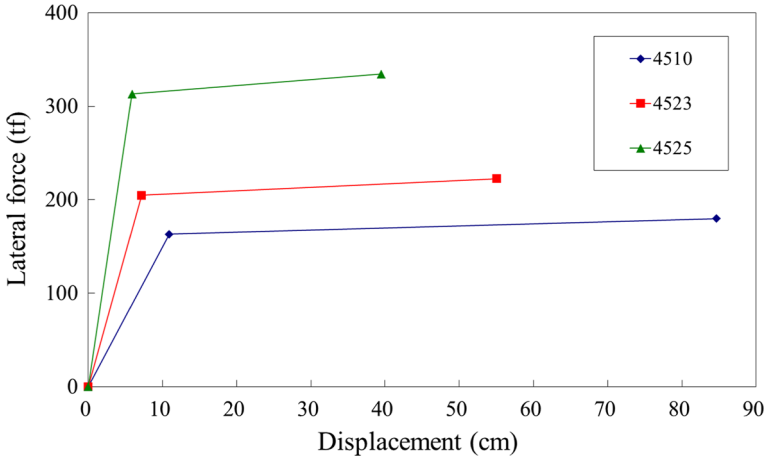

Fig. 11 Performance curves of the selected RC piers

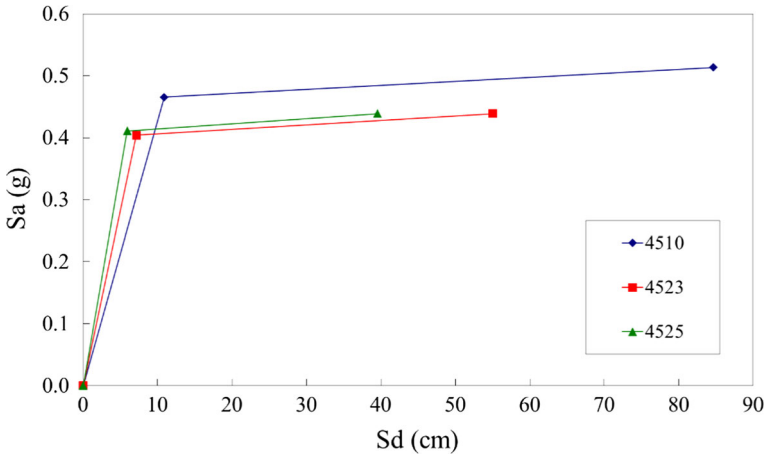

Fig. 12 Capacity spectrum of each selected RC pier

reaches damage level IV, the seismic capacity decreases significantly and should be repaired or retrofitted as soon as possible. Restated, the continuous use of the damaged structure without any repair or retrofit would not be allowed. Therefore, this case study focuses on the reliability function for the serviceability of a damaged structure, which represents the non-exceedance probability of the damage level III.

The time history of acceleration recorded in Chi–Chi earthquake (name of the station is TCU074 and located in Puli of Nantou, which is about 10 km far from the epicenter of Chi–Chi earthquake) and is modified to be compatible with the response spectral acceleration for the site, which are generated using formulas in Taiwan's seismic design code (MOI 2005). On the basis of the aftershock information of Chi–Chi earthquake, the simulation of aftershocks is proceeded in this case study. Additionally, the simulation interval of aftershocks is set at seven days (1 week).

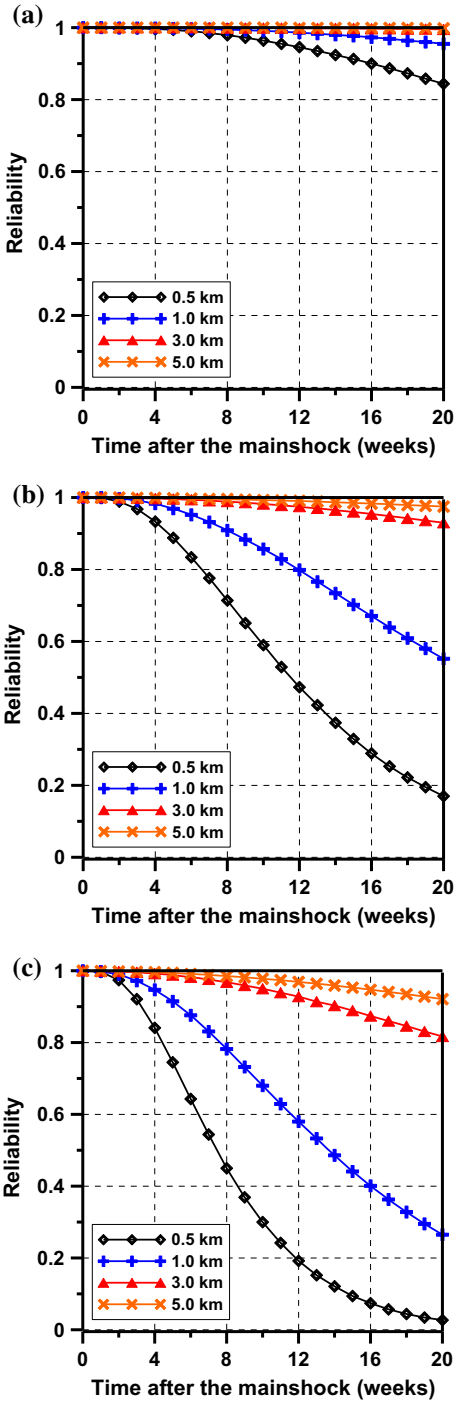

Fig. 13 Reliability of the serviceability for the selected RC piers with mainshock-induced damage level I considering various occurrence ranges of aftershocks. **a** RCP-4510, **b** RCP-4523, and **c** RCP-4525

For the selected RC piers, when the specified damage state induced by the mainshock is set at damage level I, Fig. 13 shows the reliability of the serviceability under various occurrence ranges of aftershocks. One can also set the acceptable value of the reliability to derive the service period after the mainshock. Taking RCP-4525 as an example, when the acceptable value of reliability is set at 0.50 and location of aftershocks is uniformly distributed in the range of 0.5 km from the structure's site, the serviceability-related service period is about 7 weeks from the mainshock. In Fig. 14, except for RCP-4525 and location of aftershocks uniformly distributed in the range of 1.0 km from the structure's site, post-mainshock service periods for other RC piers are almost longer than 20 weeks. Especially for RCP-4510, regardless of the condition setting of aftershocks, its serviceability-related service period is longer than 20 weeks. Restated, it is allowed to continue using the structure until the aftershock terminating. Additionally, under the same condition setting of the mainshock-induced damage state (level I) and location of aftershocks (1.0 km), Fig. 14 shows that the seismic performance of RCP-4510 is higher than other two RC piers obviously.

Finally, to determine the effect of the mainshock-induced damage state on post-mainshock service periods, we assume mainshock-induced damage states for the selected RC piers are set at level I, level II, and level III, respectively. Figure 15 shows the serviceability-related reliability corresponding to various damage levels assuming that the location of aftershocks is uniformly distributed in the range of 1.0 km from the structure's site. Taking RCP-4525 for an example, when the acceptable reliability value is set at 0.50, post-mainshock service periods are 14 (mainshock-induced damage state: level I), 10 (mainshock-induced damage state: level II), and 4 (mainshock-induced damage state: level III) weeks (Fig. 15), respectively. Additionally, compared to RCP-4525 and RCP-4523 (post-mainshock service periods are >20 (mainshock-induced damage state: level I), 17 (mainshock-induced damage state: level II), and 7 (mainshock-induced damage state: level III) weeks), RCP-4510's post-mainshock service periods are longer 20 weeks. Because the aftershock in Chi–Chi earthquake lasts about 20 weeks, RCP-4510 can still function with reliable serviceability in the post-mainshock/earthquake. This information can help engineers to arrange post-mainshock maintenance strategies for RC piers in the same region with high seismic hazard of the aftershock in an earthquake.

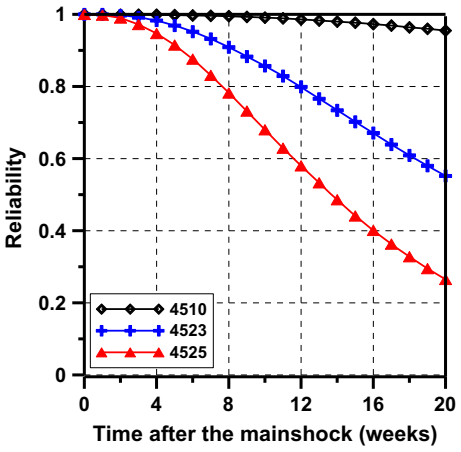

Fig. 14 Reliability of the serviceability for the selected RC piers with mainshock-induced damage level I

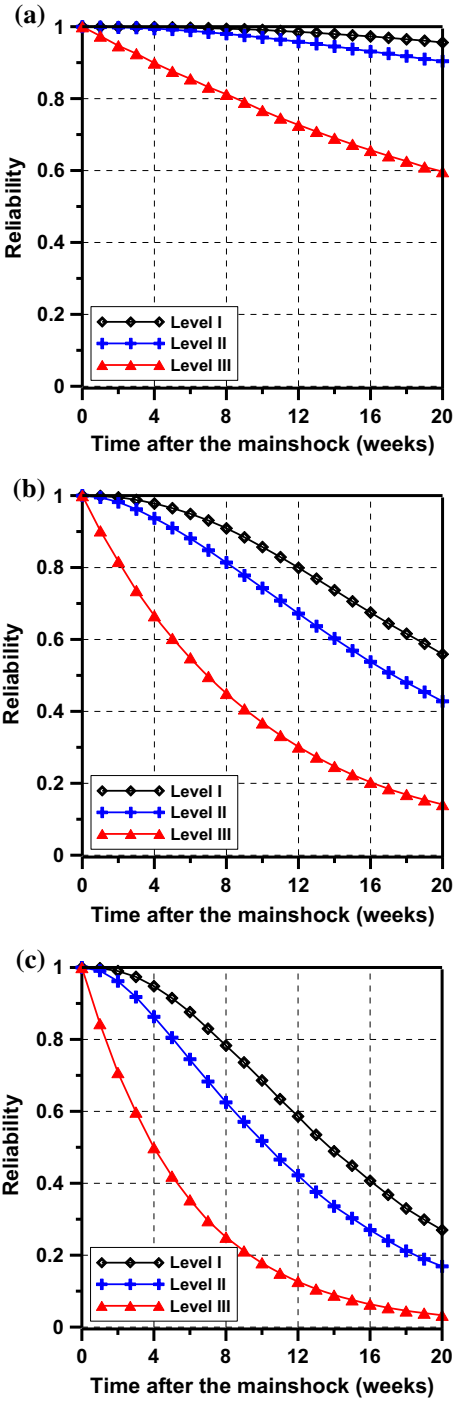

Fig. 15 Reliability of the serviceability for the selected RC piers with various damage levels induced by the mainshock. **a** RCP-4510, **b** RCP-4523, and **c** RCP-4525

5 Conclusions

This study used the experimental data of several column specimens with various failure modes (flexural, flexural-shear, and shear failure) to conclude reduction factors of seismic capacity for RC columns with various failure modes. Additionally, this study performed the nonlinear dynamic analysis for the RC column specimens with the flexural failure. Engineers can use these suggested reduction factors of seismic capacity to evaluate the residual seismic capacity for damaged RC columns conservatively and quickly in the post-mainshock inspection of seismic performance. For mainshock-damaged RC piers, the proposed seismic reliability assessment method provides useful information which can help engineers to comprehend their serviceability in a specified post-mainshock period. Via reliability functions of post-mainshock service periods, an owner of, or investor in, an RC structure can comprehend the cumulative damage effect induced by the aftershock on maintenance planning. Restated, one must consider this information when designing maintenance strategies after the mainshock in a disastrous earthquake. However, this study used the statistical data of Chi–Chi earthquake to proceed the case study. The proposed procedure can also be applied to other targets to arrange the post-mainshock maintenance. Additionally, in the future, the accuracy of simulated results can be improved with the supplement of the reliable data, e.g., uncertainties of aftershock location and structural properties.

Acknowledgements The authors would like to thank the National Science Council of the Republic of China, Taiwan, for financially supporting this research under Contract No. 101-2221-E-011-130-MY3.

References

Ang A, Tang W (1984) Probability concepts in engineering planning and design, vol 2: decision, risk and reliability. Wiley, New York

ATC (1996) Seismic evaluation and retrofit of concrete buildings. ATC-40 report, Applied Technology Council, Redwood City, California, USA

Campbell KW (1981) Near-source attenuation of peak horizontal acceleration. Bull Seism Soc Am 71:2039–2070

Chiu CK (2014a) Reliability-based service life assessment for deteriorating reinforced concrete buildings considering the effect of cumulative damage. Struct Infrastruct Eng 10(9):1101–1118

Chiu CK (2014b) Service life assessment for deteriorating RC buildings considering the effect of cumulative damage. In: Furuta H, Frangopol DM, Akiyama M (eds) Life-cycle of structural systems design, assessment, maintenance and management, pp 1607–1614. http://ir.lib.ntust.edu.tw/handle/987654321/53013

Chiu CK, Chi KN, Lin FC (2014a) Experimental investigation on the shear crack development of shear-critical high-strength reinforced concrete beams. J Adv Concr Technol 12:223–238

Chiu CK, Lyu YC, Jean WY (2014b) Probability-based damage assessment for reinforced concrete bridge columns considering the corrosive and seismic hazards in Taiwan. Nat Hazards 71(3):2143–2164

Choi H, Nakano Y, Takahashi N (2006) Residual Seismic Performance of RC frames with unreinforced block wall based on crack widths. First European conference on earthquake engineering and seismology (a joint event of the 13th ECEE & 30th General Assembly of the ESC) Geneva, Switzerland, 3–8 Sept 2006, Paper Number:748

Clough RW, Benuska KL, Wilson EL (l965) Inelastic earthquake response of tall buildings. In: Proceedings of the 3rd world conference on earthquake engineering, 22 January–1 February, Auckland and Wellington, New Zealand: New Zealand National Committee on Earthquake Engineering Care of New Zealand Institution of Engineers, vo1 II, Session II, pp 68–89

Jalayer F, Asprone D, Prota A, Manfredi G (2011) A decision support system for post-earthquake reliability assessment of structures subjected to aftershocks: an application to L'Aquila earthquake, 2009. Bull Earthq Eng 9(4):997–1014

JBDPA (2001) Guideline for post-earthquake damage evaluation and rehabilitation of RC buildings. The Japan Building Disaster Prevention Association, Tokyo
Kumar R, Gardoni P (2014) Renewal theory-based life-cycle analysis of deteriorating engineering systems. Struct Saf 50:94–102
Kumar R, Cline D, Gardoni P (2015) A stochastic framework to model deterioration in engineering systems. Struct Saf 53:36–43
Maeda M, Bunno M (2001) Post-earthquake damage evaluation for RC buildings based on residual seismic capacity in structural members. In: The third US–Japan workshop on performance based seismic design of reinforced concrete building structures, Seattle, pp 157–169
Maeda M, Kang DE (2009) Post-earthquake damage evaluation of reinforced concrete buildings. J Adv Concr Technol 7(3):327–335
Maeda M, Nakano Y, Lee KS (2004) Post-earthquake damage evaluation for R/C buildings based on residual seismic capacity. In: The 13th world conference on earthquake engineering, Vancouver
MOI (2005) Seismic design code for buildings. Minister of the Interior of Taiwan, Taiwan
MOTC (2011) Forecast of the largest magnitude in aftershock sequence. Ministry of Transportation and Communications of Taiwan, Taipei
Nakano Y, Maeda M, Kuramoto H, Murakami M (2004) Guideline for post-earthquake damage evaluation and rehabilitation of RC buildings in Japan. In: Proceedings of the 13th World Conference on Earthquake Engineering, Vancouver, Canada
Takeda T, Sozen MA, Nilson NN (1972) Reinforced concrete response to simulated earthquake. J Struct Eng (ASCE) 96(12):2557–2573
Utsu T (1961) Statistical study on the occurrence of aftershocks. Geophys Mag 30:521–605
Xue Q, Wu CW, Chen CC, Chou WY (2009) Post-earthquake loss assessment based on structural component damage inspection for residential RC buildings. Eng Struct 31:2947–2953
Yeo GL, Cornell CA (2009) Building life-cycle cost analysis due to mainshock and after shock occurrences. Struct Saf 31:396–408